# Spin-flavor structure of chiral-odd generalized parton distributions in the large-$N_c$ limit

P. Schweitzer[1,2,*] and C. Weiss[3,†]

[1] *Institute for Theoretical Physics, Tübingen University, Auf der Morgenstelle 14, 72076 Tübingen, Germany*

[2] *Department of Physics, University of Connecticut, Storrs, Connecticut 06269, USA*

[3] *Theory Center, Jefferson Lab, Newport News, Virginia 23606, USA*

(Received 6 July 2016; published 5 October 2016)

We study the spin-flavor structure of the nucleon's chiral-odd generalized parton distributions (transversity GPDs) in the large-$N_c$ limit of QCD. In contrast to the chiral-even case, only three combinations of the four chiral-odd GPDs are nonzero in the leading order of the $1/N_c$ expansion: $\bar{E}_T = E_T + 2\widetilde{H}_T, H_T$, and $\widetilde{E}_T$. The degeneracy is explained by the absence of spin-orbit interactions correlating the transverse momentum transfer with the transverse quark spin. It can also be deduced from the natural $N_c$ scaling of the quark-nucleon helicity amplitudes associated with the GPDs. In the GPD $\bar{E}_T$ the flavor-singlet component $u + d$ is leading in the $1/N_c$ expansion, while in $H_T$ and $\widetilde{E}_T$ it is the flavor-nonsinglet components $u - d$. The large-$N_c$ relations are consistent with the spin-flavor structure extracted from hard exclusive $\pi^0$ and $\eta$ electroproduction data, if it is assumed that the processes are mediated by twist-3 amplitudes involving the chiral-odd GPDs and the chiral-odd pseudoscalar meson distribution amplitudes.

DOI: 10.1103/PhysRevC.94.045202

## I. INTRODUCTION

Generalized parton distributions (GPDs) have become an essential tool in the study of nucleon structure in QCD; see Refs. [1–4] for a review. They parametrize the nucleon matrix elements of quark and gluon light-ray operators at nonzero momentum transfer and unify the concepts of parton density and elastic form factor. As such they provide a comprehensive description of the nucleon's quark and gluon single-particle structure and its spin-flavor dependence. At twist-2 level the nucleon's quark structure is described by four chiral-even (quark helicity-conserving) and four chiral-odd (quark helicity-flipping) GPDs; the number corresponds to that of independent quark-nucleon helicity amplitudes [5]. The chiral-even GPDs reduce to the usual unpolarized and helicity-polarized quark parton distribution functions (PDFs) in the limit of zero momentum transfer. These GPDs appear in the collinear QCD factorization of amplitudes of hard exclusive processes such as deeply virtual Compton scattering [6–8] and exclusive meson electroproduction with longitudinal photon polarization [9] and can be accessed experimentally in this way. The chiral-odd GPDs reduce to the quark transversity PDFs in the limit of zero momentum transfer. Relating these GPDs to hard exclusive processes has proved to be challenging. The chiral-odd GPDs decouple from single vector meson electroproduction at leading twist in all orders in perturbative QCD due to the chirality requirements for massless fermions [10]. It has been argued that the chiral-odd GPDs could be probed in diffractive electroproduction of two mesons with large invariant mass (rapidity gap) [11–13], but the proposed kinematics is difficult to access and no data are presently available.

Recent theoretical work suggests that hard exclusive electroproduction of pseudoscalar mesons ($\pi^0,\eta,\pi^+$) may be described by a hard scattering mechanism involving the twist-2 chiral-odd nucleon GPDs and the twist-3 chiral-odd meson distribution amplitude [14–17]; see Ref. [18] for a summary. A large chiral-odd distribution amplitude is induced by the dynamical breaking of chiral symmetry in QCD, and its normalization can be determined model-independently in terms of the chiral condensate [15,16]. While the mechanism is formally power-suppressed and no strict factorization has been established at this level, the pseudoscalar production amplitudes have been calculated in a modified hard scattering approach, which implements suppression of large-size $q\bar{q}$ configurations in the meson through the QCD Sudakov form factor [15,16]. The results agree well with the $\pi^0$ and $\eta$ electroproduction data from the JLab CLAS experiment at 6 GeV incident energy, regarding both the absolute cross sections and the dominance of transverse photon amplitudes ($L/T$ ratio) inferred from the azimuthal-angle-dependent response functions [19,20]. A tentative spin-flavor separation of the chiral-odd GPDs has been performed by combining data in $\pi^0$ and $\eta$ electroproduction using the different sensitivity of the two channels [20]. Further dedicated experiments in pseudoscalar meson electroproduction are planned with the JLab 12 GeV upgrade.

In order to interpret the pseudoscalar meson production data and assess the potential of this method for GPD studies, it is necessary to gain more insight into the properties of the chiral-odd GPDs from other sources. In contrast to the chiral-even GPDs, in the chiral-odd case neither the zero-momentum transfer limit of the GPDs (transversity PDFs) nor the local operator limit (form factors of local tensor operators) correspond to structures that are easily measurable, so that little useful information can be obtained in this way. The transversity PDFs can be extracted from polarization observables in semi-inclusive deep-inelastic scattering, and in principle also from dilepton production in polarized proton-proton collisions, but the methods have large theoretical and experimental uncertainties; see Refs. [21–23] and references

*peter.schweitzer@phys.uconn.edu

†weiss@jlab.org

 ©2016 American Physical Society

therein. The form factors of local tensor operators, which constrain the lowest $x$ moments of the chiral-odd GPDs, have been calculated in lattice QCD [24] and in various dynamical models of nucleon structure; see Refs. [25,26] for a review. The $x$-dependent chiral-odd GPDs have been studied in quark bound-state models of nucleon structure [27–32]. Besides these estimates not much is known about the properties of the chiral-odd GPDs.

The limit of a large number of colors in QCD (large-$N_c$ limit) provides a powerful model-independent method for studying the spin-flavor structure of nucleon matrix elements [33–35]. The conceptual basis and practical implementation of this approach have been described extensively in the literature, see Ref. [36] for a review. In the large-$N_c$ limit QCD becomes semiclassical, and baryons can be described by mean field solutions in an effective theory formulated in terms of meson fields [34]. While the dynamics remains complex and cannot be solved exactly, and the form of the mean field solution is not known, qualitative insights can be obtained by exploiting its known symmetry properties [37,38]. The resulting scaling relations for baryon mass splittings, meson-baryon coupling constants, electromagnetic and axial form factors, and other observables are generally in good agreement with experiment [36,39–42]. In matrix elements of quark bilinear operators (vector or axial vector currents, tensor operators) the large-$N_c$ limit identifies leading and subleading spin-flavor components and implies a parametric hierarchy in nucleon structure. The approach can be extended to parton densities [43,44], where it suggests a large flavor asymmetry of the polarized antiquark distribution $\Delta\bar{u} - \Delta\bar{d}$, as supported by the recent BNL Relativistic Heavy Ion Collider $W^{\mp}$ production data [45,46]. The $N_c$ scaling of chiral-odd quark distributions (transversity PDFs) was considered in Refs. [47–49], and that of local chiral-odd operators (tensor charges) in Refs. [50,51], in the context of calculations in the chiral-quark soliton model of the large-$N_c$ nucleon. A general method for the $1/N_c$ expansion of GPDs was described in Ref. [1] and applied to chiral-even GPDs.

In this article we study the spin-flavor structure of the nucleon's chiral-odd GPDs in the large-$N_c$ limit and discuss its implications. We derive the $N_c$ scaling of the chiral-odd GPDs using the method of Ref. [1] and observe interesting differences between the chiral-even and chiral-odd cases. We show that the findings can be explained as the result of natural $N_c$ scaling of the nucleon-quark helicity amplitudes associated with the chiral-odd GPDs [5,53]. The spin-flavor structure obtained in the large-$N_c$ limit is found to be consistent with that observed in an analysis of the JLab CLAS $\pi^0$ and $\eta$ hard exclusive electroproduction data, assuming that these processes are mediated by twist-3 chiral-odd meson distribution amplitudes.

The present study generalizes previous results in the $1/N_c$ expansion of chiral-even GPDs [1], quark transversity distributions [47–49], and matrix elements of local chiral-odd operators [50] and uses the formal apparatus developed in these earlier works. The description of the apparatus and explicit quotation of chiral-even results is intended only to make the present article readable. An intuitive and independent derivation of the $N_c$ scaling of the chiral-odd GPDs based on nucleon-quark helicity amplitudes was given in Ref. [52].

## II. CHIRAL-ODD GPDS

GPDs parametrize the nonforward nucleon matrix elements of QCD light-ray operators of the general form [1–4]

$$\mathcal{M}(\Gamma) = P^+ \int \frac{dz^-}{2\pi} e^{ixP^+z^-} \langle N,p'|\bar{\psi}(-z/2) \times \Gamma\psi(z/2)|N,p\rangle|_{z^+=0,z_T=0}, \tag{1}$$

where $P \equiv \frac{1}{2}(p' + p)$ is the average nucleon four-momentum, $z$ is a light-like distance, and the four-vectors are described by their light-cone components $z^{\pm} = (z^0 \pm z^3)/\sqrt{2}, z_T = (z^1,z^2)$, etc. The light-ray operators generally contain a gauge link along the light-like path defined by $z$, which we do not indicate for brevity. $\Gamma$ denotes a generic matrix in spinor indices and defines the spin structure of the operator. In the chiral-even case the relevant spinor matrices are $\Gamma = \gamma^+$ and $\gamma^+\gamma_5$, and the matrix elements are parametrized as

$$\mathcal{M}(\gamma^+) = \bar{u}'\left[\gamma^+ H + \frac{i\sigma^{+j}\Delta_j}{2M_N}E\right]u, \tag{2}$$

$$\mathcal{M}(\gamma^+\gamma_5) = \bar{u}'\left[\gamma^+\gamma_5\widetilde{H} + \frac{\gamma_5\Delta^+}{2M_N}\widetilde{E}\right]u. \tag{3}$$

In the chiral-odd case the spinor matrix is $\Gamma = i\sigma^{+j} (j = 1,2)$, and the matrix element is parametrized as [5]

$$\mathcal{M}(i\sigma^{+j}) = \bar{u}\left[i\sigma^{+j}H_T + \frac{P^+\Delta^j - \Delta^+P^j}{M_N^2}\widetilde{H}_T + \frac{\gamma^+\Delta^j - \Delta^+\gamma^j}{2M_N}E_T + \frac{\gamma^+P^j - P^+\gamma^j}{M_N}\widetilde{E}_T\right]u. \tag{4}$$

Here $u \equiv u(p,\lambda)$ and $u' \equiv u(p',\lambda')$ are the bispinors of the initial and final nucleon (the choice of polarization states will be specified later) and $\Delta \equiv p' - p$ is the four-momentum transfer. The GPDs $H \equiv H(x,\xi,t)$, etc., are functions of the average quark plus momentum fraction $x$, the plus momentum transfer to the quark, $\xi \equiv -\Delta^+/(2P^+) = (p - p')^+/(p + p')^+$, and the invariant momentum transfer to the nucleon, $t \equiv \Delta^2$. For brevity we do not indicate the dependence of the GPDs on the normalization scale of the QCD operator.

The quark fields in Eq. (1) carry flavor indices (suppressed for brevity), and the correlator is generally a matrix in flavor space. The usual flavor-diagonal GPDs are obtained with the operator

$$H^f \leftrightarrow \bar{\psi}_f \ldots \psi_f \quad (f = u,d), \tag{5}$$

where the matrix element refers to the proton state. Alternatively one may consider the isoscalar and isovector combinations $u \pm d$ of operators and GPDs. In the following we shall specify the flavor and isospin structure of the matrix elements as needed.

The chiral-even and odd GPDs satisfy certain symmetry relations in $\xi$, resulting from time reversal invariance,

$$\mathrm{GPD}(x,-\xi,t) = \begin{cases} +\mathrm{GPD}(x,\xi,t) & \text{for GPD} = H,\widetilde{H},E,\widetilde{E},H_T,\widetilde{H}_T,E_T, \\ -\mathrm{GPD}(x,\xi,t) & \text{for GPD} = \widetilde{E}_T. \end{cases} \tag{6}$$

Integration over the variable $x$ reduces the light-ray operators in Eq. (1) to local operators. In the chiral-even case these are the vector and axial vector currents, so that the $x$ integrals (or first moments) of the GPDs coincide with the electromagnetic and axial form factors of the nucleon [6]. In the chiral-odd case the local operator is the tensor operator $\bar{\psi}(0)i\sigma^{\mu\nu}\psi(0)$, and the first moments of the GPDs are

$$\int_{-1}^{1} dx\{H_T,\widetilde{H}_T,E_T,\widetilde{E}_T\}(x,\xi,t) = \{H_T(t),\widetilde{H}_T(t),E_T(t),0\}, \tag{7}$$

where $H_T(t),\widetilde{H}_T(t)$, and $E_T(t)$ are the nucleon's tensor form factors [with the same flavor structure as the GPDs, cf. Eq. (5)]. The vanishing of the first moment of $\widetilde{E}_T$ is a consequence of the antisymmetry in $\xi$, Eq. (6); its higher moments are nonzero. The higher $x$ moments of chiral-even and odd GPDs are polynomials in $\xi$ (generalized form factors).

In the limit of zero momentum transfer (forward limit) the chiral-even GPDs $H$ and $\widetilde{H}$ reduce, respectively, to the unpolarized and helicity PDFs, $H(x,\xi=0,t=0) = f_1(x)$ and $\widetilde{H}(x,\xi=0,t=0) = g_1(x)$. The GPDs $E$ and $\widetilde{E}$ are also non-zero in the forward limit but do not reduce to any known PDFs, as these GPDs correspond to nucleon helicity-flip components of the matrix element (see Sec. IV). The chiral-odd GPD $H_T$ reduces in the forward limit to the transversity PDF,

$$H_T(x,\xi=0,t=0) = h_1(x). \tag{8}$$

Its first moment is known as the nucleon's tensor charge. Because the local tensor operator is not a conserved current, the tensor charge is scale-dependent and cannot directly be related to low-energy properties of the nucleon. The forward limit of the chiral-odd GPDs $\widetilde{H}_T$ and $E_T$ is not related to any known PDFs, while $\widetilde{E}_T$ vanishes in the forward limit again due to its antisymmetry in $\xi$, Eq. (6). Other aspects of the GPDs, such as their partonic interpretation, are described in Refs. [1–4].

In Eqs. (2)–(4) the GPDs appear as invariant amplitudes, arising from a particular decomposition of the matrix elements into bilinear forms in the nucleon spinors. In applications to exclusive pseudoscalar meson production processes it is natural to introduce the combination

$$\bar{E}_T \equiv E_T + 2\widetilde{H}_T \tag{9}$$

of the chiral-odd GPDs, which corresponds to a different invariant decomposition of the matrix element Eq. (4) [16]. An alternative representation of the GPDs as nucleon-quark helicity amplitudes will be described in Sec. IV.

## III. CHIRAL-ODD GPDS IN LARGE-$N_c$ LIMIT

In the large-$N_c$ limit the nucleon mass scales as $M_N \sim N_c$, while the nucleon size remains stable, $\sim N_c^0$. The $1/N_c$ expansion of GPDs is performed in a class of frames where the initial and final nucleon move with three-momenta $p^k,p'^k \sim N_c^0\,(k=1,2,3)$ and have energies $p^0,p'^0 = M_N + O(1/N_c)$, which implies an energy and momentum transfer $\Delta^0 \sim N_c^{-1},\Delta^k \sim N_c^0$, and thus

$$\Delta^i \sim N_c^0\,(i=1,2), \quad \xi \sim N_c^{-1}, \quad |t| \sim N_c^0. \tag{10}$$

In the partonic variable $x$ one considers the parametric region

$$x \sim N_c^{-1}, \tag{11}$$

corresponding to nonexceptional longitudinal momenta of the quarks and antiquarks relative to the slowly moving nucleon, $xM_N \sim (\text{nucleon size})^{-1} \sim N_c^0$. Likewise, it is assumed that the normalization scale of the light-ray operator is $\sim N_c^0$, so that the typical quark transverse momenta are $\sim N_c^0$. Equation (11) corresponds to the intuitive picture of a nucleon consisting of $N_c$ "valence" quarks and a "sea" of $\mathcal{O}(N_c)$ quark-antiquark pairs, with the quarks/antiquarks carrying on average a fraction $\sim 1/N_c$ of the nucleon's light-cone momentum. Altogether, the $N_c$-scaling relations for GPDs can then be expressed in the form

$$\mathrm{GPD}(x,\xi,t) \sim N_c^k \times \text{function}\,(N_c x,N_c\xi,t), \tag{12}$$

where the scaling exponent $k$ depends on the GPD in question and the isospin component $(u+d,u-d)$ and can be established on general grounds, while the scaling function on the right-hand side is stable in the large-$N_c$ limit and can only be determined in specific dynamical models.

A practical method for performing the $1/N_c$ expansion of baryon matrix elements of quark bilinear operators was given in Refs. [1,54], using collective quantization of an abstract mean-field solution with known symmetry properties. One considers a generic correlator of the form

$$\langle B',\boldsymbol{p}'|\overline{\psi}_{\alpha' f'}(x')\psi_{\alpha f}(x)|B,\boldsymbol{p}\rangle, \tag{13}$$

where the quark fields are at space-time points $x$ and $x'$, and $(\alpha,\alpha')$ and $(f,f')$ are the Dirac spinor and flavor indices. We restrict ourselves to the $SU(2)$ flavor sector and assume exact isospin symmetry. The baryon states are characterized by their momenta $\boldsymbol{p}$ and $\boldsymbol{p}'$, and spin-isospin quantum numbers $B \equiv \{S,S_3,T,T_3\}$ and $B' \equiv \{S',S_3',T',T_3'\}$, and normalized such that

$$\langle B',\boldsymbol{p}'|B,\boldsymbol{p}\rangle = 2p^0(2\pi)^3\delta^{(3)}(\boldsymbol{p}'-\boldsymbol{p})\delta_{BB'}, \quad \delta_{BB'} \equiv \delta_{SS'}\delta_{S_3S_3'}\delta_{TT'}\delta_{T_3T_3'}. \tag{14}$$

For simplicity we do not specify the color indices of the quark fields in Eq. (13) and do not indicate the gauge link (in the case of GPDs the gauge link can be eliminated by choosing the light-cone gauge; in a more general case it can be included explicitly by an appropriate redefinition of the quark fields [49]). One evaluates the correlator Eq. (13) starting with the expectation value of the bilinear operator in the localized mean field characterizing the large-$N_c$ baryon ("soliton"), centered at the origin,

$$\langle\overline{\psi}_{\alpha' f'}(x')\psi_{\alpha f}(x)\rangle = \mathcal{F}(x'^0 - x^0, \boldsymbol{x}', \boldsymbol{x})_{\alpha f;\alpha' f'}. \tag{15}$$

While the specific form of the function $\mathcal{F}$ depends on dynamics and can only be determined in models, its symmetry properties in the large-$N_c$ limit can be established on general grounds. In leading order of $1/N_c$ the baryon mean field is static (time-independent), so that the correlator depends only on the relative time $x'^0 - x^0$. Most importantly, the mean field intertwines spatial and isospin degrees of freedom ("hedgehog symmetry") [37], so that a rotation in flavor space by an $SU(2)$ matrix $R$, and a simultaneous spatial rotation with a rotation matrix $O(R)$ and spin rotation $S(R)$, leave the correlator Eq. (15) invariant,

$$S(R)_{\alpha\beta} R_{fg} \mathcal{F}(x'^0 - x^0, O(R)\boldsymbol{x}', O(R)\boldsymbol{x})_{\beta g,\beta', g'} R^{-1}_{g' f'} S(R^{-1})_{\beta'\alpha'} = \mathcal{F}(x'^0 - x^0, \boldsymbol{x}', \boldsymbol{x})_{\alpha f;\alpha' f'}, \tag{16}$$

where

$$O^{ji}(R) \equiv \tfrac{1}{2}\mathrm{tr}[R^{-1}\tau^j R \tau^i] \quad (i,j = 1,2,3), \tag{17}$$

and $O(R)\boldsymbol{x}'$ and $O(R)\boldsymbol{x}$ denote the rotation of the three-vectors $\boldsymbol{x}'$ and $\boldsymbol{x}$ with the matrix $O(R)$. The mean field breaks translational and rotational/isorotational invariance and does not correspond to states of definite momentum and spin/isospin quantum numbers. The matrix element between baryon states of definite momentum and spin/isospin is obtained by quantizing the collective motion in coordinate and isospin space and projecting on states with appropriate quantum numbers. In this way one obtains a representation of the baryon matrix element Eq. (13) in the form [34,54]

$$\langle B', \boldsymbol{p}'|\overline{\psi}_{\alpha' f'}(x')\psi_{\alpha f}(x)|B, \boldsymbol{p}\rangle = 2M_B N_c \int \mathrm{d}R\, \phi^*_{B'}(R)\phi_B(R) \times \int \mathrm{d}^3X\, e^{i(\boldsymbol{p}-\boldsymbol{p}')\cdot \boldsymbol{X}} R_{fg}\mathcal{F}(x'^0 - x^0, \boldsymbol{x}' - \boldsymbol{X}, \boldsymbol{x} - \boldsymbol{X})_{\alpha g;\alpha' g'}(R^{-1})_{g' f'} + \cdots, \tag{18}$$

where the dots indicate subleading terms in $1/N_c$ and $M_B \sim N_c$ is the baryon mass (note that $M_{B'} = M_B$ in leading order of $1/N_c$). The integral over the position of the center of the mean field, $\boldsymbol{X}$, with wave functions $\exp(-i\,\boldsymbol{p}'\boldsymbol{X})$ and $\exp(i\,\boldsymbol{p}\boldsymbol{X})$ projects the correlator Eq. (15) on baryon states with momenta $\boldsymbol{p}$ and $\boldsymbol{p}'$. The integral over the flavor rotation $R$ with rotational wave functions $\phi_B(R)$ and $\phi^*_{B'}(R)$ projects on baryon states with spin/isospin quantum numbers $B$ and $B'$. The hedgehog symmetry of the mean field [cf. Eq. (16)] implies that the baryon states occur in representations with equal spin and isospin, $S = T$, and the rotational wave functions are given by the Wigner finite rotation matrices as [1]

$$\phi_B(R) \equiv \phi^{S=T}_{S_3 T_3}(R) = \sqrt{2S+1}(-1)^{T+T_3} D^{S=T}_{-T_3, S_3}(R). \tag{19}$$

Using Eq. (18) one can evaluate the matrix element of any bilinear quark operator in leading nonvanishing order of the $1/N_c$ expansion. The hedgehog symmetry of the mean field, Eq. (16), restricts the spin-isospin structures emerging from the rotational integral and determines the $N_c$ scaling of the spin-flavor components of the matrix element. These relations depend on the specific form of the operator considered.

The chiral-even GPDs were evaluated in this way in Ref. [1]. Here the operators are the light-ray operators of Eq. (1) with the chiral-even spinor matrices $\Gamma = \gamma^+$ and $\Gamma = \gamma^+\gamma^5$, cf. Eq. (2). It is instructive to perform the integration over collective coordinates in Eq. (18) in two steps. In the first step one considers the correlator integrated over the coordinate $\boldsymbol{X}$ but not yet over rotations, i.e., projected on momentum states but not yet on spin/isospin states. This correlator describes the GPDs of a large-$N_c$ baryon that has not yet been projected on spin-isopsin states ("soliton GPDs"). In the chiral-even case it was found to be of the form [1]

$$M_N \int \frac{\mathrm{d}z^-}{2\pi} e^{ixP^+z^-} \langle \mathrm{sol}, \boldsymbol{p}'|\bar{\psi}_{f'}(-z/2) \begin{Bmatrix}\gamma^+ \\ \gamma^+\gamma_5\end{Bmatrix} \psi_f(z/2)|\mathrm{sol}, \boldsymbol{p}\rangle\Big|_{z^+=0, z_T=0} = \begin{Bmatrix} \delta_{f'f} H_{\mathrm{sol}} - \dfrac{i\varepsilon^{3jk}\Delta^j}{2M_N} D^k_{f'f} E_{\mathrm{sol}} \\ D^3_{f'f}\widetilde{H}_{\mathrm{sol}} - \dfrac{\Delta^3\Delta^j}{(2M_N)^2} D^j_{f'f}\widetilde{E}_{\mathrm{sol}} \end{Bmatrix}, \tag{20}$$

where $H_{\mathrm{sol}}, E_{\mathrm{sol}}, \widetilde{H}_{\mathrm{sol}}$, and $\widetilde{H}_{\mathrm{sol}}$ are functions of $x, \xi$, and $t$, and [cf. Eq. (17)]

$$D^i_{f'f} \equiv D^i_{f'f}(R) \equiv \tfrac{1}{2}(\tau^j)_{f'f} O^{ji}(R). \tag{21}$$

This expression embodies the hedgehog symmetry expressed by Eq. (16): the flavor-singlet structure $\propto \delta_{f'f}$ is independent of the rotation matrix $R$ defining the orientation of the soliton, while the flavor-nonsinglet structures $\propto (\tau^j)_{f'f}$ are accompanied by rotation matrices and coupled with the spatial directions defined by the light-ray operator ($z$ direction) and the momentum transfer $\boldsymbol{\Delta}$. In the second step one then projects the soliton matrix element on spin-isospin states by performing the integral over rotations, using

$$\int \mathrm{d}R\, \phi^{*S'=T'=1/2}_{S'_3 T'_3}(R)\phi^{S=T=1/2}_{S_3 T_3}(R) \begin{Bmatrix} 1 \\ O^{ji}(R)\end{Bmatrix} = \begin{Bmatrix} \delta_{S'_3 S_3}\delta_{T'_3 T_3} \\ -\frac{1}{3}(\sigma^i)_{S'_3 S_3}(\tau^j)_{T'_3 T_3}\end{Bmatrix}. \tag{22}$$

The resulting nucleon matrix elements can be expressed in a transparent form by introducing a shorthand matrix notation for the nucleon spin components,

$$\sigma^0 \equiv \sigma^0(S_3',S_3) \equiv \delta_{S_3',S_3}, \quad \sigma^i \equiv \sigma^i(S_3',S_3) \equiv (\sigma^i)_{S_3',S_3}, \tag{23}$$

and correspondingly for the quark flavor components,

$$\tau^0 \equiv \tau^0(f',f) \equiv \delta_{f'f}, \quad \tau^j \equiv \tau^j(f',f) \equiv (\tau^j)_{f'f}. \tag{24}$$

In this notation the nucleon matrix elements become (we consider the proton with $T_3' = T_3 = 1/2$)

$$\mathcal{M}(\gamma^+) = \sigma^0\tau^0 H_{\rm sol} + \frac{i(\boldsymbol{\Delta}\times\boldsymbol{\sigma})^3\tau^3}{3(2M_N)} E_{\rm sol}, \tag{25}$$

$$\mathcal{M}(\gamma^+\gamma_5) = -\frac{\sigma^3\tau^3}{3}\widetilde{H}_{\rm sol} + \frac{\Delta^3\boldsymbol{\Delta}\cdot\boldsymbol{\sigma}\tau^3}{3(2M_N)^2}\widetilde{E}_{\rm sol}. \tag{26}$$

Equations (25) and (26) express the spin-flavor symmetry characteristic of the large-$N_c$ limit: the spin-singlet matrix element is also a flavor-singlet, and the spin-nonsinglet one is a flavor-nonsinglet. They also allow one to determine the explicit $N_c$ scaling of the chiral-even GPDs. The $N_c$ scaling of the soliton GPDs in Eq. (20) follows from the fact that the spatial size of the mean field is $\sim N_c^0$, and from the kinematic prefactors emerging from the $1/N_c$ expansion of the spin structures in the matrix element, and is given by [cf. Eq. (12)]

$$\{H_{\rm sol}, E_{\rm sol}, \widetilde{H}_{\rm sol}, \widetilde{E}_{\rm sol}\}(x,\xi,t) \sim \left\{N_c^2, N_c^3, N_c^2, N_c^4\right\} \times \text{function } (N_c x, N_c\xi, t). \tag{27}$$

The $N_c$ scaling of the leading flavor components of the chiral-even nucleon GPDs is thus obtained as [1]

$$\{H^{u+d}, E^{u-d}, \widetilde{H}^{u-d}, \widetilde{E}^{u-d}\}(x,\xi,t) \sim \left\{N_c^2, N_c^3, N_c^2, N_c^4\right\} \times \text{function } (N_c x, N_c\xi, t). \tag{28}$$

The respective opposite flavor combinations are suppressed by one order in $1/N_c$, i.e., $H^{u-d} \sim N_c$, etc.

We now apply this method to the chiral-odd GPDs and derive their $N_c$ scaling. The calculations are performed in complete analogy to the chiral-even case described above [1]. Using the specific decomposition of the chiral-odd correlator Eq. (4) and performing the $1/N_c$ expansion of the components, we obtain the chiral-odd soliton GPDs as [cf. Eqs. (20) and (21)]

$$\begin{aligned} M_N \int \frac{dz^-}{2\pi} e^{ixP^+z^-} \langle \text{sol}, \boldsymbol{p}'|\bar\psi_{f'}(-z/2) i\sigma^{+j} \\ \times\psi_f(z/2)|\text{sol},\boldsymbol{p}\rangle|_{z^+=0,z_T=0} \\ = \frac{\Delta^j}{2M_N}\delta_{f'f}\bar{E}_{T,\rm sol} + i\varepsilon^{3jk}D^k_{f'f}H_{T,\rm sol} \\ + \frac{i\varepsilon^{jkl}\Delta^k}{2M_N}D^l_{f'f}\widetilde{E}_{T,\rm sol}. \end{aligned} \tag{29}$$

The hedgehog symmetry is again manifest in the structure of the right-hand side. Notice that the large-$N_c$ matrix element has only three independent structures, and that the GPDs $E_T$ and $\widetilde{H}_T$ appear only in the combination $\bar{E}_T$, Eq. (9). Projecting on nucleon states ($T_3' = T_3 = 1/2$) we obtain, in the matrix notation of Eqs. (25), (26) ($\boldsymbol{e}_3$ denotes the unit vector in the $z$-direction),

$$\begin{aligned} \mathcal{M}(i\sigma^{+j}) = \sigma^0\tau^0\frac{\Delta^j}{2M_N}\bar{E}_{T,\rm sol} + \frac{(\boldsymbol{e}_3\times\boldsymbol{\sigma})^j\tau^3}{3}H_{T,\rm sol} \\ - \frac{(\boldsymbol{\Delta}\times\boldsymbol{\sigma})^j\tau^3}{3(2M_N)}\widetilde{E}_{T,\rm sol} \quad (j=1,2). \end{aligned} \tag{30}$$

The result again expresses the spin-flavor symmetry characteristic of the large-$N_c$ limit. The $N_c$ scaling of the chiral-odd soliton GPDs is found to be

$$\{\bar{E}_{T,\rm sol}, H_{T,\rm sol}, \widetilde{E}_{T,\rm sol}\}(x,\xi,t) \sim \left\{N_c^3, N_c^2, N_c^3\right\} \times \text{function } (N_c x, N_c\xi, t). \tag{31}$$

We can thus identify the leading flavor components of the chiral-odd nucleon GPDs and determine their $N_c$ scaling,

$$\left\{\bar{E}_T^{u+d}, H_T^{u-d}, \widetilde{E}_T^{u-d}\right\}(x,\xi,t) \sim \left\{N_c^3, N_c^2, N_c^3\right\} \times \text{function } (N_c x, N_c\xi, t). \tag{32}$$

The respective other flavor components are suppressed by at least one power of $1/N_c$,

$$\left\{\bar{E}_T^{u-d}, H_T^{u+d}, \widetilde{E}_T^{u+d}\right\}(x,\xi,t) \sim \left\{N_c^2, N_c, N_c^2\right\} \times \text{function } (N_c x, N_c\xi, t). \tag{33}$$

These results confirm our earlier intuitive derivation of the $N_c$ scaling using helicity amplitudes [52].

The large-$N_c$ limit exposes an interesting difference between the chiral-even and chiral-odd quark correlation functions in the nucleon, regarding the number of independent nucleon spin structure components, as described by the matrices $\sigma^0$ and $\sigma^i (i = 1,2,3)$. It can be exhibited by projecting the spin matrices $\sigma^i (i = 1,2,3)$ on the orthogonal three-vectors $\boldsymbol{e}_3$ (the direction defined by the light-ray operator), $\boldsymbol{\Delta}_T \equiv \boldsymbol{\Delta} - (\boldsymbol{e}_3\cdot\boldsymbol{\Delta})\boldsymbol{e}_3$ (the component of $\boldsymbol{\Delta}$ orthogonal to $\boldsymbol{e}_3$), and

$$\boldsymbol{n}_T \equiv \boldsymbol{e}_3 \times \boldsymbol{\Delta} \tag{34}$$

(the normal vector of the plane defined by $\boldsymbol{e}_3$ and $\boldsymbol{\Delta}_T$, or the complement of $\boldsymbol{\Delta}_T$ in the transverse plane). In the chiral-even correlators Eqs. (25) and (26) one finds that all spin structures

$$\sigma^0, \quad \boldsymbol{e}_3\cdot\boldsymbol{\sigma}, \quad \boldsymbol{\Delta}_T\cdot\boldsymbol{\sigma}, \quad \boldsymbol{n}_T\cdot\boldsymbol{\sigma} \tag{35}$$

are nonzero and occur with four independent coefficient functions. In the chiral-odd correlators Eq. (30), however, the transverse nucleon spin structures $\boldsymbol{\Delta}_T\cdot\boldsymbol{\sigma}$ and $\boldsymbol{n}_T\cdot\boldsymbol{\sigma}$ occur only in the combination

$$\boldsymbol{e}_3\times\boldsymbol{\sigma}, \tag{36}$$

which *does not depend on the direction of the transverse momentum* $\boldsymbol{\Delta}_T$, and there are only three independent coefficient functions. One sees that the reason why there are only three independent chiral-odd GPDs is that the large-$N_c$ nucleon does not correlate the direction of the transverse quark spin (as defined by the light-ray operator with $\sigma^{+j}$) with that of the transverse nucleon spin (as contained in the spin structures $\boldsymbol{e}_3\times\boldsymbol{\sigma}$ of the matrix element) through the nucleon's transverse momentum transfer. The absence of such spin-orbit interactions is specific to the leading order of the

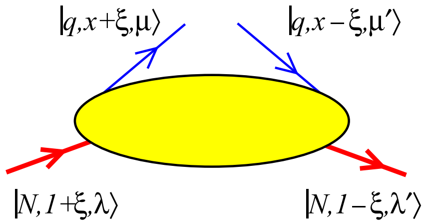


FIG. 1. Representation of GPDs in the region $\xi < x < 1$ as nucleon-quark helicity amplitudes. In the nucleon and quark states (denoted as $N,q$) the second label denotes the fraction of the light-cone plus momentum $P^+$ carried by the particle, and the third label denotes the light-cone helicity.

$1/N_c$ expansion, and we expect that higher-order corrections will remove the degeneracy of the transverse spin structures.

### IV. CHIRAL-ODD GPDS AS HELICITY AMPLITUDES

Further insight into the different behavior of chiral-even and odd GPDs in the large-$N_c$ limit can be gained by considering the representation of the GPDs as partonic helicity amplitudes [53]. This representation most naturally appears in the region $\xi < x < 1$, where the GPDs describe the amplitude for the "emission" by the nucleon of a quark with plus momentum fraction $x+\xi$ and subsequent "absorption" of a quark with $x-\xi$ (see Fig. 1). In the region $-1 < x < -\xi$ the GPDs describe the emission and absorption of an antiquark, while in $-\xi < x < \xi$ they describe the emission of a quark-antiquark pair by the nucleon. We do not need to consider these regions separately in the subsequent arguments.

The partonic helicity amplitudes are defined by a correlator of the form of Eq. (1), in which the nucleon spin states are described as light-front helicity states and the quark spinor matrices are chosen as projectors on quark light-front helicity states:

$$A_{\lambda'\mu',\lambda\mu} = P^+ \int \frac{dz^-}{2\pi} e^{ixP^+z^-} \langle N,p',\lambda'|\overline{\psi}(-z/2)\Gamma_{\mu'\mu} \times \psi(z/2)|N,p,\lambda\rangle|_{z^+=0,z_T=0}, \quad (37)$$

where $\lambda(\lambda')$ are the light-front helicities of the initial (final) nucleon and $\mu(\mu')$ those of the initial (final) quark [53]. It is convenient to work in a reference frame where the light-cone direction is chosen as the $z$ axis and the initial and final nucleon momenta $\boldsymbol{p}$ and $\boldsymbol{p}'$ lie in the $x$-$z$ plane. The spinor matrices for the light-front helicity-conserving (chiral-even) and light-front helicity-flipping (chiral-odd) amplitudes are then given by [5]

$$\Gamma_{\pm\pm} = \frac{1}{4}\gamma^+(1\pm\gamma_5), \quad (38)$$

$$\Gamma_{\pm\mp} = \frac{i}{4}\sigma^{+1}(\pm 1-\gamma_5) = \frac{i}{4}(\pm\sigma^{+1}+i\sigma^{+2}). \quad (39)$$

Flavor components of the amplitudes can be defined in analogy to those of the correlator Eq. (1) and will be specified below. The helicity-conserving amplitudes are related to the chiral-even GPDs as

$$A_{++,++} = \frac{1}{2}\sqrt{1-\xi^2}\left(H+\widetilde{H}-\frac{\xi^2}{1-\xi^2}(E+\widetilde{E})\right), \quad (40a)$$

$$A_{-+,-+} = \frac{1}{2}\sqrt{1-\xi^2}\left(H-\widetilde{H}-\frac{\xi^2}{1-\xi^2}(E-\widetilde{E})\right), \quad (40b)$$

$$A_{++,-+} = \frac{1}{2}\delta_t(\xi\widetilde{E}-E), \quad (40c)$$

$$A_{-+,++} = \frac{1}{2}\delta_t(\xi\widetilde{E}+E), \quad (40d)$$

while the helicity-flipping amplitudes are related to the chiral-odd GPDs as

$$A_{++,+-} = \delta_t\left(\widetilde{H}_T+\frac{1-\xi}{2}(E_T+\widetilde{E}_T)\right), \quad (41a)$$

$$A_{-+,--} = \delta_t\left(\widetilde{H}_T+\frac{1+\xi}{2}(E_T-\widetilde{E}_T)\right), \quad (41b)$$

$$A_{++,--} = \sqrt{1-\xi^2}\left(H_T+\delta_t^2\widetilde{H}_T-\frac{\xi^2}{1-\xi^2}E_T + \frac{\xi}{1-\xi^2}\widetilde{E}_T\right), \quad (41c)$$

$$A_{-+,+-} = \sqrt{1-\xi^2}\delta_t^2\widetilde{H}_T, \quad (41d)$$

where the "kinematic" prefactor $\delta_t$ is defined as

$$\delta_t = \text{sign}(P^+\Delta^1-\Delta^+P^1)\frac{\sqrt{t_0-t}}{2M_N}, \quad -t_0 = \frac{4M_N^2\xi^2}{1-\xi^2}, \quad (42)$$

in which $-t_0$ is the minimal value of $-t$ for the given value of $\xi$. There are four linearly independent amplitudes in each sector; the other four amplitudes in each sector can be obtained from those in Eqs. (40a)–(40d) and (41a)–(41d) by the parity relation [5]

$$A_{-\lambda'-\mu',-\lambda-\mu} = (-)^{\lambda'-\mu'-\lambda+\mu}A_{\lambda'\mu',\lambda\mu}. \quad (43)$$

Altogether, there are eight linearly independent helicity amplitudes, corresponding to the total number of chiral-even and chiral-odd GPDs (or invariant amplitudes).

It is instructive to study the $N_c$ scaling of the partonic helicity amplitudes. The "natural" scaling of the individual helicity amplitudes for a given quark flavor ($f=u,d$) is

$$A^f_{\lambda'\mu',\lambda\mu} \sim N_c^2, \quad (44)$$

which is understood with the arguments $x,\xi$, and $t$ scaling as in Eq. (12). One power of $N_c$ originates from the normalization of the nucleon states in Eq. (14), because $P^0 \sim N_c$, and another power of $N_c$ from the implicit summation over the color indices in the light-ray operators. Combinations of amplitudes corresponding to definite isospin transitions ($u+d,u-d$) can vanish in leading order of the $1/N_c$ expansion due to the symmetries of the mean field solution (cf. Sec. III) and can have a lower scaling exponent. Using the results of Ref. [1] and Sec. III for the $N_c$ scaling of the GPDs we can now identify the leading and subleading helicity amplitudes. For the chiral-even amplitudes one obtains

$$A^{u+d}_{++,++} = \tfrac{1}{2}H^{u+d}, \quad A^{u-d}_{++,++} = \tfrac{1}{2}(\widetilde{H}^{u-d}-\xi^2\widetilde{E}^{u-d}), \quad (45a)$$

$$A^{u+d}_{-+,-+} = \tfrac{1}{2} H^{u+d}, \quad A^{u-d}_{-+,-+} = \tfrac{1}{2}(-\widetilde{H}^{u-d} + \xi^2 \widetilde{E}^{u-d}), \tag{45b}$$

$$A^{u+d}_{++,-+} = 0, \quad A^{u-d}_{++,-+} = \tfrac{1}{2}\delta_t(\xi \widetilde{E}^{u-d} - E^{u-d}), \tag{45c}$$

$$A^{u+d}_{-+,++} = 0, \quad A^{u-d}_{-+,++} = \tfrac{1}{2}\delta_t(\xi \widetilde{E}^{u-d} + E^{u-d}). \tag{45d}$$

The expressions correspond to the leading order of the $1/N_c$ expansion, i.e., they are accurate at the natural order $\mathcal{O}(N_c^2)$. It is understood that all non-zero amplitudes receive corrections of order $\mathcal{O}(N_c)$. The amplitudes that vanish do so at order $\mathcal{O}(N_c^2)$, and generically have corrections of order $\mathcal{O}(N_c)$. Notice that in the specific frame chosen here in the large-$N_c$ limit the kinematic factors simplify as

$$\delta_t = \frac{\Delta^1}{2M_N}, \quad \xi = -\frac{\Delta^3}{2M_N}. \tag{46}$$

One notices that two pairs of the chiral-even amplitudes are degenerate (up to an overall sign) at $\mathcal{O}(N_c^2)$, and two other amplitudes vanish at this order. The content of Eqs. (45a)–(45d) becomes more transparent when considering linear combinations of the chiral-even amplitudes,

$$A^{u+d}_{++,++} + A^{u+d}_{-+,-+} = H^{u+d}, \tag{47a}$$

$$A^{u-d}_{++,++} - A^{u-d}_{-+,-+} = \widetilde{H}^{u-d} - \xi^2 \widetilde{E}^{u-d}, \tag{47b}$$

$$A^{u-d}_{-+,++} + A^{u-d}_{++,-+} = \xi \delta_t \widetilde{E}^{u-d}, \tag{47c}$$

$$A^{u-d}_{-+,++} - A^{u-d}_{++,-+} = \delta_t E^{u-d}. \tag{47d}$$

This representation shows that there are four independent combinations of helicity amplitudes that appear in leading order of the $1/N_c$ expansion, which are unambiguously associated with the four leading spin-flavor components of the chiral-even GPDs. As a consequence, each of the four chiral-even GPDs has a leading flavor component: $u + d$ in $H$, and $u - d$ in $\widetilde{H}, E$, and $\widetilde{E}$.

The situation is different in the case of chiral-odd helicity amplitudes. Using the results of the $1/N_c$ expansion of Sec. III we obtain the following scaling behavior of the chiral-odd helicity amplitudes at $\mathcal{O}(N_c^2)$:

$$A^{u+d}_{++,+-} = \tfrac{1}{2}\delta_t \bar{E}^{u+d}_T, \quad A^{u-d}_{++,+-} = \tfrac{1}{2}\delta_t \widetilde{E}^{u-d}_T, \tag{48a}$$

$$A^{u+d}_{-+,--} = \tfrac{1}{2}\delta_t \bar{E}^{u+d}_T, \quad A^{u-d}_{-+,--} = -\tfrac{1}{2}\delta_t \widetilde{E}^{u-d}_T, \tag{48b}$$

$$A^{u+d}_{++,--} = 0, \quad A^{u-d}_{++,--} = H^{u-d}_T + \xi \widetilde{E}^{u-d}_T, \tag{48c}$$

$$A^{u+d}_{-+,+-} = 0, \quad A^{u-d}_{-+,+-} = 0. \tag{48d}$$

Again, we obtain a more transparent representation by considering the linear combinations

$$A^{u+d}_{++,+-} + A^{u+d}_{-+,--} = \delta_t \bar{E}^{u+d}_T, \tag{49a}$$

$$A^{u-d}_{++,+-} - A^{u-d}_{-+,--} = \delta_t \widetilde{E}^{u-d}_T, \tag{49b}$$

$$A^{u-d}_{++,--} = H^{u-d}_T + \xi \widetilde{E}^{u-d}_T, \tag{49c}$$

$$A^{u\pm d}_{-+,+-} = 0. \tag{49d}$$

One sees that in the chiral-odd case one amplitude vanishes completely: $A_{-+,+-} = 0$ for *both* flavor combinations $u + d$ and $u - d$. As a result, there are only three linearly independent amplitudes that are nonzero in leading order of the $1/N_c$ expansion. This reflects the results of Sec. III, where it was found that only three independent GPDs are present in the large-$N_c$ nucleon, see Eqs. (29) and the following equations. Notice that, because $A_{-+,+-}$ is related exclusively to the GPD $\widetilde{H}_T$ and this amplitude vanishes for any flavor combination, it is not possible to separate the linear combination of the GPDs $\bar{E}_T = E_T + 2\widetilde{H}_T$ in leading order of the $1/N_c$ expansion.

The amplitude $A_{-+,+-}$ is unique in that it corresponds to a *double-helicity-flip transition* with angular momentum exchange $\Delta J = 2$ between the active quark and the nucleon, i.e., the nucleon and quark helicities are flipped in opposite directions. It is natural that for this amplitude both flavor combinations vanish in leading order of the $1/N_c$ expansion. Because of the spin-flavor symmetry implied by the large-$N_c$ limit the transition with $\Delta J = 2$ should be accompanied by isospin transfer $\Delta T = 2$, which is impossible with a quark one-body operator. This could be proved more formally by expanding the GPDs in powers of the transverse momentum transfer, such that they can be represented by matrix elements of local operators (containing total derivatives) at zero transverse momentum transfer, and classifying the resulting local operators according to the spin-flavor symmetry implied by the large-$N_c$ limit. The collective quantization procedure of Sec. III [1,54] implements this symmetry through the hedgehog symmetry of the mean field, Eq. (16).

It is interesting to note that the vanishing of the amplitude $A_{-+,+-}$ in leading order of the $1/N_c$ expansion can also be derived from large-$N_c$ consistency arguments. The latter are analogous to the unitarity requirements imposed on meson-baryon scattering amplitudes, from which one can derive specific relations between meson-baryon coupling constants [42,55]. In fact, a nonvanishing amplitude $A^{u\pm d}_{-+,+-} \sim N_c^2$ (for any of the flavor combinations) would imply that $\widetilde{H}^{u\pm d} \sim N_c^4$. Inserting this scaling behavior into $A_{++,+-}$ or $A_{-+,--}$ would imply that these amplitudes should scale as $\sim N_c^3$, which contradicts the natural scaling Eq. (44).[1]

In the discussion here we have inferred the $N_c$ scaling of the helicity amplitudes from that of the GPDs (or invariant amplitudes). Alternatively one may consider the large-$N_c$ correlators, Eqs. (25), (26), and (30), directly in the particular frame $\mathbf{\Delta} = (\Delta^1, 0, \Delta^3)$ and determine the helicity amplitudes from there. For reference we present in the Appendix the expressions for the correlators in that frame. They show explicitly the degeneracy of the transverse spin structure of the chiral-odd correlator noted in Sec. III [cf. Eqs. (35) and (36)], which is the cause of the reduced number of independent

[1]Although the partonic helicity amplitudes are not strictly physical, they enter into the description of cross sections of certain exclusive processes with quark helicity flip. If some of the amplitudes were to scale as $\sim N_c^3$ it is plausible that this would violate positivity constraints for the cross sections of some hypothetical physical scattering processes. Whether such an argument could be applied to chiral-odd GPDs remains an interesting question for further study. Positivity constraints for chiral-odd GPDs were discussed in Ref. [56].

chiral-odd GPDs viz. helicity amplitudes in leading order of the $1/N_c$ expansion.

## V. FLAVOR STRUCTURE FROM PSEUDOSCALAR MESON PRODUCTION DATA

It is interesting to compare our results with preliminary data from the JLab CLAS exclusive pseudoscalar meson production experiments [19,20] (cf. comments in Sec. I). Analysis of the azimuthal-angle dependent response functions shows that $|\sigma_{LT}| \ll |\sigma_{TT}|$, which indicates dominance of the twist-3 amplitudes, involving the chiral-odd GPDs $H_T$ and $\bar{E}_T = E_T + 2\widetilde{H}_T$, over the twist-2 amplitudes involving the chiral-even GPD $\widetilde{E}$. A preliminary flavor decomposition was performed assuming dominance of the twist-3 amplitudes and combining the data on $\pi^0$ and $\eta$ production, in which the $u$ and $d$ quark GPDs enter with different relative weight. Results show opposite sign of the exclusive amplitudes $\langle H_T^u\rangle$ and $\langle H_T^d\rangle$, which is consistent with the leading appearance of the flavor-nonsinglet $H_T^{u-d}$ in the $1/N_c$ expansion. (Here $\langle\cdots\rangle$ denotes the integral over $x$ of the GPD, weighted with the meson wave function, hard process amplitude, and Sudakov form factor [16].) The results also suggest same sign of $\langle \bar{E}_T^u\rangle$ and $\langle \bar{E}_T^d\rangle$, which is again consistent with the leading appearance of the flavor-singlets $E_T^{u+d}$ and $\widetilde{H}_T^{u+d}$ in the $1/N_c$ expansion. These findings should be interpreted with two caveats: (a) the errors in the experimental extraction of $\langle H_T\rangle$ and $\langle \bar{E}_T\rangle$ are substantial; (b) the $1/N_c$ expansion predicts only the scaling behavior, not the absolute magnitude of the individual flavor combinations, cf. Eq. (12).

It is encouraging that the flavor structure of the amplitudes extracted from the $\pi^0$ and $\eta$ electroproduction data is consistent with the pattern predicted by the $1/N_c$ expansion. Our findings further support the idea that pseudoscalar meson production at $x_B \gtrsim 0.1$ and $Q^2 \sim$ few GeV$^2$ is governed by the twist-3 mechanism involving the chiral-odd GPDs.

## VI. DISCUSSION AND OUTLOOK

The large-$N_c$ limit reveals interesting characteristic differences between the nucleon matrix elements of chiral-even and chiral-odd light-ray operators. While in the chiral-even case four GPDs (or invariant amplitudes) are nonzero in the leading order of the $1/N_c$ expansion, in the chiral-odd case only three independent GPDs appear, due to the absence of spin-orbit interactions correlating the transverse quark spin with the transverse momentum transfer to the nucleon. In the equivalent representation of GPDs as nucleon-quark helicity amplitudes, the same happens due to the vanishing of the double helicity-flip amplitude in the leading order of $1/N_c$. These conclusions are model-independent and do not rely on any assumptions regarding the internal dynamics giving rise to the partonic structure.

The leading order of the $1/N_c$ expansion predicts the scaling behavior of the leading flavor combinations in the GPDs $\bar{E}_T = E_T + 2\widetilde{H}_T, H_T$, and $\widetilde{E}_T$. Interestingly, the hard exclusive amplitudes in the twist-3 mechanism involve exactly these three combinations of GPDs, so that the large-$N_c$ predictions can be confronted with experimental observables.

The $N_c$-scaling relations of the chiral-odd GPDs described here generalize earlier results for the $N_c$ scaling of the nucleon's transversity PDFs [47,48], tensor charges [50], and tensor form factors [51]. We note that the lattice QCD calculations of Ref. [24] of the tensor form factors $A_{T10}(t) = H_T(t) \equiv \int dx\, H_T(x,\xi,t)$ show opposite sign for $u$ and $d$ flavors, while those for $\bar{B}_{T10}(t) = \bar{E}_T(t) \equiv \int dx\, \bar{E}_T(x,\xi,t)$ show same sign for $u$ and $d$ flavors, in agreement with the leading-order large-$N_c$ relations Eq. (32). The flavor structure of $\bar{E}_T(t)$ at large $N_c$ was also studied in the bag model calculation of Ref. [28] and agrees with the general result.

In the present study we have considered the leading nonvanishing order of the $1/N_c$ expansion of the chiral-odd nucleon matrix elements. Extension to subleading order requires principal considerations and technical improvements. At subleading order the mean-field approximation to the large-$N_c$ correlation functions Eq. (18) must include the effects of the finite velocity of the soliton collective (iso)rotations, $\Omega \sim N_c^{-1}$. At the same time one must reconsider the choice of nucleon spinors in the invariant decomposition of the matrix elements, Eqs. (2) and (3), as the apparent size of "relativistic corrections" to a given invariant amplitude may depend on the choice of nucleon spinors. The choice should be guided by the symmetries of the leading-order approximation and incorporate corrections through a Foldy-Wouthuysen transformation.

It would be interesting to calculate the chiral-odd GPDs in dynamical models that consistently implement the $N_c$ scaling, such as the chiral quark-soliton model. Such calculations would allow one to calculate also the scaling functions in the large-$N_c$ relations, Eq. (12), and supplement the scaling studies with dynamical information. $N_c$ scaling can also be implemented in calculations of peripheral GPDs (at impact parameters $b \sim M_\pi^{-1}$) in chiral effective field theory [57].

## ACKNOWLEDGMENTS

In this study we greatly benefited from discussions with D. Diakonov, V. Petrov, P. Pobylitsa, and M. Polyakov during earlier joint work. This material is based upon work supported by the U.S. Department of Energy, Office of Science, Office of Nuclear Physics under Contract No. DE-AC05-06OR23177. This work was supported by the U.S. National Science Foundation under Contract No. 1406298, and by the Deutsche Forschungsgemeinschaft (Grant No. VO 1049/1).

## APPENDIX: LARGE-$N_c$ CORRELATORS IN HELICITY FRAME

In this Appendix we express the nucleon-quark helicity amplitudes in the large-$N_c$ limit directly in terms of the large-$N_c$ correlators Eqs. (25), (26), and (30). To this end we consider the correlators in the specific frame where the nucleon momenta lie in the $x$-$z$ plane, $\mathbf{\Delta} = (\Delta^1,0,\Delta^3)$, and with the momentum components given by Eq. (46). The chiral-even correlators Eqs. (25), (26) take the form [in the shorthand notation of Eq. (23)]

$$\mathcal{M}(\gamma^+) = \sigma^0\tau^0 H_{\text{sol}} + \frac{i\sigma^2\tau^3}{3}\delta_t E_{\text{sol}}, \quad \text{(A1)}$$

$$\mathcal{M}(\gamma^+\gamma_5) = -\frac{\sigma^1\tau^3}{3}\delta_t\xi\widetilde{E}_{\text{sol}} + \frac{\sigma^3\tau^3}{3}(\xi^2\widetilde{E}_{\text{sol}} - \widetilde{H}_{\text{sol}}). \quad \text{(A2)}$$

We now use that (a) the Dirac matrices $\gamma^+$ and $\gamma^+\gamma_5$ are the sum and difference of the quark helicity projectors,

$$\left.\begin{matrix}\gamma^+ \\ \gamma^+\gamma_5\end{matrix}\right\} = 2(\Gamma_{++} \pm \Gamma_{--}); \quad \text{(A3)}$$

(b) the nucleon light-front helicity can be identified with the ordinary spin projection on the $z$-axis in leading order of the $1/N_c$ expansion; (c) the helicity amplitudes with quark helicities $--$ can be expressed in terms of those with $++$ by the parity relations Eq. (43). In this way we obtain

$$\sigma^0\tau^0 \to 2(A^{u+d}_{++,++} + A^{u+d}_{-+,-+}), \quad \text{(A4a)}$$

$$\sigma^3\tau^3 \to 2(A^{u-d}_{++,++} - A^{u-d}_{-+,-+}), \quad \text{(A4b)}$$

$$\sigma^1\tau^3 \to 2(A^{u-d}_{++,-+} + A^{u-d}_{-+,++}), \quad \text{(A4c)}$$

$$i\sigma^2\tau^3 \to 2(A^{u-d}_{++,-+} - A^{u-d}_{-+,++}), \quad \text{(A4d)}$$

in the sense that the corresponding structures in the large-$N_c$ correlators Eqs. (A1) and (A2) are to be identified with the given combination of helicity amplitudes. The content of the relations Eqs. (A4a)–(A4d) becomes identical to that of Eqs. (47a)–(47d) if one substitutes the large-$N_c$ expressions for the nucleon GPDs in terms of the soliton GPDs. The chiral-odd correlator Eq. (30) in the same representation takes the form

$$\mathcal{M}(i\sigma^{+1}) = \sigma^0\tau^0\delta_t\bar{E}_{T,\text{sol}} - \frac{\sigma^2\tau^3}{3}(H_{T,\text{sol}} + \xi\widetilde{E}_{T,\text{sol}}), \quad \text{(A5)}$$

$$\mathcal{M}(i\sigma^{+2}) = \frac{\sigma^1\tau^3}{3}(H_{T,\text{sol}} + \xi\widetilde{E}_{T,\text{sol}}) - \frac{\sigma^3\tau^3}{3}2\delta_t\widetilde{E}_{T,\text{sol}}. \quad \text{(A6)}$$

We now use that

$$i\sigma^{+1} = 2(\Gamma_{+-} - \Gamma_{-+}), \quad \text{(A7)}$$

$$i\sigma^{+2} = -2i(\Gamma_{+-} + \Gamma_{-+}), \quad \text{(A8)}$$

express the amplitudes with quark helicities $+-$ in terms of those with $-+$ using the parity relations Eq. (43), and obtain

$$\sigma^0\tau^0 \to 2(A^{u+d}_{++,+-} + A^{u+d}_{-+,--}), \quad \text{(A9a)}$$

$$\sigma^2\tau^3 \to 2i(A^{u-d}_{++,--} - A^{u-d}_{-+,+-}), \quad \text{(A9b)}$$

$$\sigma^1\tau^3 \to -2i(A^{u-d}_{++,--} + A^{u-d}_{-+,+-}), \quad \text{(A9c)}$$

$$\sigma^3\tau^3 \to -2i(A^{u-d}_{++,+-} - A^{u-d}_{-+,--}), \quad \text{(A9d)}$$

to be understood in the same sense as Eqs. (A4a)–(A4d). Again, these relations reproduce Eqs. (49a)–(49d) if we substitute the specific large-$N_c$ expressions of the nucleon GPDs in terms of the soliton GPDs.

Equations (A4a)–(A4d) exhibit the degeneracy of the large-$N_c$ correlator noted in Sec. III: the spin structures $\sigma^1$ and $\sigma^2$ occur with the same coefficient function and thus cannot be distinguished in the large-$N_c$ nucleon. This illustrates again that in leading order of the $1/N_c$ expansion there is no correlation between the transverse nucleon spin, $\sigma^1$ or $\sigma^2$, and the transverse momentum transfer, $\boldsymbol{\Delta}_T = (\Delta^1, 0)$.


[1] K. Goeke, M. V. Polyakov, and M. Vanderhaeghen, Prog. Part. Nucl. Phys. **47**, 401 (2001).
[2] M. Diehl, Phys. Rep. **388**, 41 (2003).
[3] A. V. Belitsky and A. V. Radyushkin, Phys. Rep. **418**, 1 (2005).
[4] S. Boffi and B. Pasquini, Riv. Nuovo Cim. **30**, 387 (2007).
[5] M. Diehl, Eur. Phys. J. C **19**, 485 (2001).
[6] X. D. Ji, Phys. Rev. D **55**, 7114 (1997).
[7] A. V. Radyushkin, Phys. Rev. D **56**, 5524 (1997).
[8] A. V. Belitsky, D. Müller, and A. Kirchner, Nucl. Phys. B **629**, 323 (2002).
[9] J. C. Collins, L. Frankfurt, and M. Strikman, Phys. Rev. D **56**, 2982 (1997).
[10] J. C. Collins and M. Diehl, Phys. Rev. D **61**, 114015 (2000).
[11] D. Y. Ivanov, B. Pire, L. Szymanowski, and O. V. Teryaev, Phys. Lett. B **550**, 65 (2002).
[12] R. Enberg, B. Pire, and L. Szymanowski, Eur. Phys. J. C **47**, 87 (2006).
[13] M. El Beiyad, B. Pire, M. Segond, L. Szymanowski, and S. Wallon, Phys. Lett. B **688**, 154 (2010).
[14] S. Ahmad, G. R. Goldstein, and S. Liuti, Phys. Rev. D **79**, 054014 (2009)
[15] S. V. Goloskokov and P. Kroll, Eur. Phys. J. C **65**, 137 (2010).
[16] S. V. Goloskokov and P. Kroll, Eur. Phys. J. A **47**, 112 (2011).
[17] G. R. Goldstein, J. O. G. Hernandez, and S. Liuti, J. Phys. G **39**, 115001 (2012); Phys. Rev. D **91**, 114013 (2015); arXiv:1401.0438 [hep-ph].
[18] P. Kroll, arXiv:1602.03803 [hep-ph].
[19] I. Bedlinskiy *et al.* (CLAS Collaboration), Phys. Rev. Lett. **109**, 112001 (2012); Phys. Rev. C **90**, 025205 (2014); **90**, 039901(E) (2014).
[20] V. Kubarovsky (CLAS Collaboration), Int. J. Mod. Phys. Conf. Ser. **40**, 1660051 (2016).
[21] A. Bacchetta, A. Courtoy, and M. Radici, J. High Energy Phys. 03 (2013) 119.
[22] M. Anselmino, M. Boglione, U. D'Alesio, S. Melis, F. Murgia, and A. Prokudin, Phys. Rev. D **87**, 094019 (2013).
[23] Z. B. Kang, A. Prokudin, P. Sun, and F. Yuan, Phys. Rev. D **91**, 071501 (2015).
[24] M. Gockeler *et al.* (QCDSF and UKQCD Collaborations), Phys. Rev. Lett. **98**, 222001 (2007).
[25] V. Barone, A. Drago, and P. G. Ratcliffe, Phys. Rep. **359**, 1 (2002).

[26] M. Burkardt and B. Pasquini, Eur. Phys. J. A **52**, 161 (2016).
[27] B. Pasquini, M. Pincetti, and S. Boffi, Phys. Rev. D **72**, 094029 (2005).
[28] M. Burkardt and B. Hannafious, Phys. Lett. B **658**, 130 (2008).
[29] D. Chakrabarti, R. Manohar, and A. Mukherjee, Phys. Rev. D **79**, 034006 (2009).
[30] M. Wakamatsu, Phys. Rev. D **79**, 014033 (2009).
[31] N. Kumar and H. Dahiya, Phys. Rev. D **91**, 114031 (2015).
[32] D. Chakrabarti and C. Mondal, Phys. Rev. D **92**, 074012 (2015).
[33] G. 't Hooft, Nucl. Phys. B **72**, 461 (1974).
[34] E. Witten, Nucl. Phys. B **160**, 57 (1979).
[35] S. R. Coleman and E. Witten, Phys. Rev. Lett. **45**, 100 (1980).
[36] E. E. Jenkins, Annu. Rev. Nucl. Part. Sci. **48**, 81 (1998).
[37] E. Witten, Nucl. Phys. B **223**, 433 (1983).
[38] A. P. Balachandran, V. P. Nair, S. G. Rajeev, and A. Stern, Phys. Rev. D **27**, 1153 (1983); **27**, 2772 (1983).
[39] R. F. Dashen, E. E. Jenkins, and A. V. Manohar, Phys. Rev. D **49**, 4713 (1994); **51**, 2489 (1995); **51**, 3697 (1995).
[40] E. E. Jenkins, Phys. Lett. B **315**, 441 (1993).
[41] E. E. Jenkins and R. F. Lebed, Phys. Rev. D **52**, 282 (1995).
[42] R. F. Dashen and A. V. Manohar, Phys. Lett. B **315**, 425 (1993).
[43] D. Diakonov, V. Petrov, P. Pobylitsa, M. V. Polyakov, and C. Weiss, Nucl. Phys. B **480**, 341 (1996).
[44] A. V. Efremov, K. Goeke, and P. V. Pobylitsa, Phys. Lett. B **488**, 182 (2000).
[45] M. M. Aggarwal *et al.* (STAR Collaboration), Phys. Rev. Lett. **106**, 062002 (2011).
[46] A. Adare *et al.* (PHENIX Collaboration), Phys. Rev. Lett. **106**, 062001 (2011).
[47] P. V. Pobylitsa and M. V. Polyakov, Phys. Lett. B **389**, 350 (1996).
[48] P. Schweitzer, D. Urbano, M. V. Polyakov, C. Weiss, P. V. Pobylitsa, and K. Goeke, Phys. Rev. D **64**, 034013 (2001).
[49] P. V. Pobylitsa, arXiv:hep-ph/0301236.
[50] H. C. Kim, M. V. Polyakov, and K. Goeke, Phys. Rev. D **53**, R4715(R) (1996).
[51] T. Ledwig, A. Silva, and H. C. Kim, Phys. Rev. D **82**, 034022 (2010); **82**, 054014 (2010).
[52] P. Schweitzer and C. Weiss, PoS QCDEV **2015**, 041 (2015).
[53] M. Diehl, T. Feldmann, R. Jakob, and P. Kroll, Nucl. Phys. B **596**, 33 (2001); **605**, 647 (2001).
[54] P. V. Pobylitsa and M. V. Polyakov, Phys. Rev. D **62**, 097502 (2000).
[55] J. L. Gervais and B. Sakita, Phys. Rev. Lett. **52**, 87 (1984); Phys. Rev. D **30**, 1795 (1984).
[56] M. Kirch, P. V. Pobylitsa, and K. Goeke, Phys. Rev. D **72**, 054019 (2005).
[57] C. Granados and C. Weiss, J. High Energy Phys. 06 (2016) 075; 01 (2014) 092.